View metadata, citation and similar papers at core.ac.uk

brought to you by CORE

provided by Elsevier - Publisher Connector

Carbon 109 (2016) 843–850

Contents lists available at ScienceDirect

Carbon

journal homepage: www.elsevier.com/locate/carbon

A precedent of van-der-Waals interactions outmatching Coulomb explosion

S.E. Huber [a, c], M. Gatchell [b], H. Zettergren [b], A. Mauracher [a, *]

[a] Institut für Ionenphysik und Angewandte Physik, Leopold-Franzens-Universität Innsbruck, Technikerstr. 25, A-6020 Innsbruck, Austria
[b] Department of Physics, Stockholm University, AlbaNova University Center, SE-106 91 Stockholm, Sweden
[c] Institut für Grundlagen der Technischen Wissenschaften, Leopold-Franzens-Universität Innsbruck, Technikerstr. 13, A-6020 Innsbruck, Austria

ARTICLE INFO

Article history:
Received 29 June 2016
Received in revised form
9 August 2016
Accepted 20 August 2016
Available online 26 August 2016

ABSTRACT

Fullerenes (and clusters composed of them) yield a variety of promising structural, electronic, magnetic and chemical properties, governed by their specific electronic and geometric configuration. These systems have attracted many theoretical and experimental endeavors in order to describe, explain and predict their features. The conclusive description of some specific properties has remained a challenge though, such as a sound physicochemical description of the stability of multiply charged fullerene clusters, which we explore here. We show how simple models based on classical electrostatics allow one to understand the (fragmentation) dynamics of multiply ionized fullerene aggregates without the use of elaborate and time-consuming computational quantum chemical approaches. These models successfully explain why the fullerene pentamer is the smallest dicationic cluster experimentally observed, despite its thermodynamic instability. These predictions are of importance in various fields such as cluster physics, astrochemistry, electrochemistry and solid-state chemistry.

© 2016 The Authors. Published by Elsevier Ltd. This is an open access article under the CC BY-NC-ND license (http://creativecommons.org/licenses/by-nc-nd/4.0/).

1. Introduction

Fullerene aggregates are abundant in nature in various forms [1]. The interaction of fullerenes with e.g. graphene is of great importance for its potential applications in nanotechnology [2]. Especially charged systems yield promising properties for applications in molecular electronics and biomedicine [3]. Fullerene anions and especially endohedral metallofullerenes have received substantial consideration [4]. These species are important in various scientific fields like biomedicine [5], organic photovoltaic [6] or alkali metal doped fullerides [7,8]. In outer space [9], fullerene cations are formed via photoionization in ultraviolet-light environments such as interstellar and circumstellar nebulae [10]. They act as seeds for the growth of carbonaceous species [11,12] and might have implications for the origin of life [13]. Very recently a study on the relative stability of multiply charged fullerene isomers nicely summarized properties and applications of charged fullerenes [14]. Not only multiply charged monomers have received attention, but also multiply charged clusters of fullerenes. These species are of interest because they bridge the gap between isolated fullerenes and fullerene crystals (fullerites) and can be used as model systems for extended structures such as carbon nanotubes [15,16]. Dicationic fullerene clusters have been produced via charge transfer reactions from highly charged Xe cations [17]. Due to the long-range interaction between neutral fullerene clusters and the highly charged Xe cations the ionization process is very gentle and the smallest dication observed was the fullerene pentamer. Dianionic fullerene clusters have been observed in the ultra-cold environment of superfluid helium droplets [18]. There, helium droplets were doped with clusters of fullerenes and then negatively charged via charge transfer from helium anions [19]. Although these systems are different from the cationic systems from a chemical point of view, also here the smallest observable dianion was the pentamer.

In this article we present how basic considerations of electrostatics and dispersion allow one to understand and predict the stability of multiply charged van-der-Waals (vdW) oligomers at low temperatures, which we exemplify for the case of doubly charged fullerene clusters. We use two simple approaches that reduce the complex many-body systems to their essentials. In our crudest ansatz, the geometrical structures of the fullerenes are entirely omitted leaving behind chargeable and polarizable point particles located on the corners of regular polyhedra (polygons in the simplest cases), to which we hence refer as the Point Charges on

* Corresponding author.
E-mail address: andreas.mauracher@uibk.ac.at (A. Mauracher).

http://dx.doi.org/10.1016/j.carbon.2016.08.056
0008-6223/© 2016 The Authors. Published by Elsevier Ltd. This is an open access article under the CC BY-NC-ND license (http://creativecommons.org/licenses/by-nc-nd/4.0/).

Polyhedra (PCP) model. In a second step, replacement of the fullerenes by ideally conducting metal spheres reintroduces the spatial extent of the cluster constituents. This second model is referred to as the Charged Sphere (CS) model. In both models solving the complex many-body problem of the underlying quantum-chemical system, i.e. the electronic Schrödinger equation, is replaced by simple classical force field evaluations. This is done by using a two-body potential for the vdW interactions derived from Density Functional Theory (DFT) in combination with fundamental electrostatic expressions. The metallic properties of a fullerene are in general well understood [20], although there have been disputes in the past [21,22], to which our study also contributes to some extent. As electrostatic and dispersive forces and associated energies are reasonably described by analytical functions, there is no need for expensive electronic structure calculations in our models. Instead, just the knowledge of the cluster geometry and simple energy evaluations are required to predict the stability of the multiply charged clusters. For the DFT calculations, to which we compare the PCP and CS models, we applied a decomposition ansatz of the total energy which allowed us to obtain very accurate results concerning both the electrostatic and the dispersive interaction. This is a prerequisite to handle the delicate energy balance. Details are supplied in the following section on the used models and methods.

2. Modeling and methods

2.1. PCP and CS model

In the PCP model, the total interaction energy between the fullerenes, which are modeled as polarizable point particles (located on the corners of regular polyhedra or polygons for equilibrium geometries; the term equilibrium geometries refers to the DFT optimized neutral geometries for the remainder of this work), is written as a sum of contributions to the total energy due to vdW interactions, Coulomb repulsion, polarization, and dipole-dipole interactions:

$$E_{tot} = E_{vdW} + E_{Coulomb} + E_{polarization} + E_{dipole-dipole} \quad (1)$$

The vdW interaction energy is a sum of pairwise interaction energies over all pairs of point particles in the respective system. The vdW interaction energy of a pair of point particles is determined via interpolation of the potential energy surface (PES) of the neutral C_{60} dimer obtained from the DFT calculations (see below and the Supplementary information provided online).

In this model, the point charges are always located at the positions of the two furthermost point particles in the respective system. The energy due to Coulomb repulsion between these two point charges is simply given by Coulomb's law:

$$E_{Coulomb} = \frac{1}{4\pi\varepsilon_0}\frac{e^2}{r}, \quad (2)$$

where ε_0 denotes the vacuum permittivity, e denotes the elementary charge and r denotes the distance between the two point charges.

The energy due to polarization of the point particles in the system is given as the sum of polarization energies of all polarized point particles in the field of the two point charges, i.e. $E_{polarization} = \sum_i E_{polarization,i}$ with i=1,…,n and n denoting the number of polarizable point particles in the system. The energy of the i-th polarizable point particle in the electric field is given by $E_{polarization,i} = -\alpha_i E^2$, where E denotes the absolute value of the electric field at the position of the polarizable point particle, $\alpha_i = 67.34$ Å^3 for neutral point particles and $\alpha_i = 76.7$ Å^3 for point charges. These values have been derived via DFT for the polarizabilities of the neutral and singly charged fullerenes, respectively. Values from the literature vary considerably between different (both experimental and theoretical) studies in the range of (76.5 ± 8)Å^3 to (88.9 ± 6)Å^3 for neutral fullerenes [23,24] and in the range of 83.7 Å^3 to 88.1 Å^3 for cationic fullerenes [25,26]. The agreement between our calculated polarizabilities and those from the literature can be regarded as reasonable, considering the rather weak dependence of the resulting energetics on these parameters, see section 3.2. The electric field due to the two point charges reads:

$$\boldsymbol{E} = \frac{e}{4\pi\varepsilon_0}\left(\frac{1}{r_1^3}\boldsymbol{r}_1 + \frac{1}{r_2^3}\boldsymbol{r}_2\right), \quad (3)$$

where $\boldsymbol{r}_1$ and $\boldsymbol{r}_2$ denote the vectors pointing from the location of charge 1 and charge 2, respectively, to the location of the polarizable point particle. For polarization of point particles at the position of the charges, only the electric field of the other charge has been taken into account.

Finally, the interaction between the various dipoles, induced by the charges 1 and 2, is given by a sum of pair-wise interactions of the form:

$$E_{dipole-dipole} = \frac{1}{4\pi\varepsilon_0 r_{12}^3}[\boldsymbol{\mu}_1\cdot\boldsymbol{\mu}_2 - 3(\boldsymbol{\mu}_1\cdot\boldsymbol{e}_{12})(\boldsymbol{\mu}_2\cdot\boldsymbol{e}_{12})], \quad (4)$$

where $\boldsymbol{e}_{12}$ denotes the unit vector pointing from the one induced dipole with dipole moment $\boldsymbol{\mu}_1 = -\alpha_1\boldsymbol{E}_1$ to the other induced dipole with dipole moment $\boldsymbol{\mu}_2 = -\alpha_2\boldsymbol{E}_2$ and r_{12} denotes the distance between the two dipoles. This term stems from the interaction between the (permanent) dipoles induced via polarization of the point particle in the field of the external charges 1 and 2. This interaction must not be mistaken with the induced-dipole-induced-dipole term already included in the vdW term obtained from the PES of the fullerene dimer evaluated at the DFT level using Grimme's latest empirical dispersion corrections (see below) modeling London dispersion interaction between the constituents of the cluster (without permanent multipole moments). However, we note that inclusion of this term yields only a very small contribution to the resulting PESs and does not affect their overall shape.

The energy expression for the interaction energy between two polarizable (charged) spheres with permittivities $\varepsilon_1 = \varepsilon_2 = \varepsilon$ used in the CS model is given by:

$$E_{int} = \frac{1}{4\pi\varepsilon_0}\left(\frac{q_A q_B}{R} - \frac{\varepsilon-1}{\varepsilon+2}\frac{q_A^2 a_B^3}{2R^2(R^2-a_B^2)} - \frac{\varepsilon-1}{\varepsilon+2}\frac{q_B^2 a_A^3}{2R^2(R^2-a_A^2)}\right), \quad (5)$$

where R denotes the center-center distance of the spheres, $a_A = a_B = a = 8.6a_0$ (chosen as such in accordance with an earlier study [20]) with a_0 denoting the Bohr radius, and q_A and q_B denote the charges on the spheres A and B. Please note that in Eq. (5), q_A and q_B are not necessarily integers (in units of elementary charge), and e.g. in the case of asymmetric dissociation of the $(C_{60})_N^{2+}$ cluster forming C_{60}^+ and $(C_{60})_{N-1}^+$, $q_A = e$ is assigned to the fullerene monomer and $q_B = e/(N-1)$ is assigned to the each of the N−1 remaining fullerenes constituting the fragment $(C_{60})_{N-1}^+$, see section 3.3. For ideally conducting metallic spheres $\varepsilon \to \infty$. In order to explore the effect of assuming dielectric instead of ideally metallic spheres we also applied the model using $\varepsilon = 5$, which is considered

to be the dielectric constant of bulk fullerite [27]. The total energy in the CS model is obtained by adding the vdW interaction energy as obtained in the PCP model, i.e. the first term in Eq. (1), to the interaction energy described by Eq. (5).

2.2. Decomposition ansatz for DFT calculations

Concerning the DFT calculations, we made use of a decomposition ansatz by noting that the total energy of the doubly charged system (referring to the geometry of the corresponding neutral *AB* though), denoted as AB^{2+}, can be written as:

$$\begin{aligned} E_{tot}\left(AB^{2+}\right) &= E_{tot}\left(AB^{2+}\right) + E_{tot}(AB) - E_{tot}(AB) \\ &= E_{tot}(AB) + \left[E_{tot}\left(AB^{2+}\right) - E_{tot}(AB)\right] \\ &= E_{tot}(AB) + {}^{2}VIE(AB), \end{aligned} \tag{6}$$

where ${}^{2}VIE(AB)$ denotes the double vertical ionization energy of the system *AB*. So far, everything is exact. However, now we approximate the total energy of the neutral system by using the density functional that we find best suited for this task and we approximate the second vertical ionization energy by using the density functional that we find best suited for that task. Using different density functionals to derive the energy balance defines our decomposition ansatz.

Furthermore, we investigate vertical ionization processes of fullerene clusters in order to evaluate the (thermodynamic) stability of fullerene dications. Therefore, the total (electronic) energies of the cations as well as of the dications are calculated at the equilibrium geometries of the respective neutral systems. The thermodynamic stability of a dicationic system with respect to Coulomb explosion into two singly charged (fullerene cluster) fragments can be determined from

$$\Delta E = E\left((C_{60})_X^+\right) + E\left((C_{60})_Y^+\right) - E\left((C_{60})_N^{2+}\right), \quad for \;\; X + Y = N. \tag{7}$$

In the case of $\Delta E < 0$, the dicationic system is thermodynamically unstable or metastable, in the case of $\Delta E > 0$ the dicationic system is thermodynamically stable.

Since we consider vertical ionization processes, Eq. (7) can be written as

$$\begin{aligned} \Delta E &= E\left((C_{60})_X\right) + E\left((C_{60})_Y\right) - E\left((C_{60})_N\right) + VIE\left((C_{60})_X\right) \\ &\quad + VIE\left((C_{60})_Y\right) - {}^{2}VIE\left((C_{60})_N\right) \\ &= \Delta BE + \Delta IE, \end{aligned} \tag{8}$$

where ${}^{2}VIE((C_{60})_N)$ is the double vertical ionization energy, i.e.

$${}^{2}VIE\left((C_{60})_N\right) = E\left((C_{60})_N^{2+}\right) - E\left((C_{60})_N\right), \tag{9}$$

$$\Delta BE = E\left((C_{60})_X\right) + E\left((C_{60})_Y\right) - E\left((C_{60})_N\right) \tag{10}$$

$$\Delta IE = VIE\left((C_{60})_X\right) + VIE\left((C_{60})_Y\right) - {}^{2}VIE\left((C_{60})_N\right) \tag{11}$$

Using now our decomposition ansatz, as introduced when discussing Eq. (6), allows us, again, to choose different density functionals for computing individually the terms ΔBE and ΔIE in Eq. (8). These density functionals should most accurately reproduce adequate experimental values, in this study the neutral binding energy of the fullerene dimer and the single as well as the second ionization energies of the fullerene monomer. Hence, we optimized the neutral fullerene dimer with various density functionals adding the D3 version of Grimme's dispersion with Becke-Johnson damping [28] where applicable and corrected for the basis set superposition error using the method of Boys and Bernardi [29]. The results are summarized in the Supplementary information provided online in Table S1. The density functionals PBE0 [30] and CAM-B3LYP [31] in conjunction with Pople's 6-31G(d) basis set [32] lead to a binding energy of 0.280 eV and 0.283 eV, which are closest to the experimental value of (0.275 ± 0.08) eV reported by Branz et al. [33]. We choose the PBE0 functional for the optimization of the fullerene monomer to the fullerene heptamer, because the performance of PBE0 is better than that of CAM-B3LYP with respect to the convergence behavior in the involved iterative self-consistent energy computations. The Cartesian coordinates of the optimized fullerene clusters can be found also in the Supplementary information accompanying this article and provided online. All calculations were performed with the Gaussian 09 suite of programs [34].

3. Results and discussion

3.1. Charge distributions upon vertical ionization

The key point here is to note the unequal charge distribution for the considered cluster sizes upon vertical ionization. Especially for clusters larger than the tetramer the two fullerenes that are farthest apart yield a substantial excess charge compared to the others, see Fig. 1. In Fig. 1, we depict the optimized geometries of cluster sizes from the neutral dimer up to the neutral heptamer as obtained by our DFT calculations. The structures in Fig. 1 also indicate the Mulliken charge distribution for the vertically doubly ionized systems. In particular, the results obtained for the larger oligomers suggest the following approach for the construction of our heuristic PCP model: Each respective fullerene's center-of-mass forms a corner on a regular polyhedron in agreement with an earlier investigation [35]. To each of these positions a polarizable point mass with the mass of a fullerene is assigned and two elementary charges are allocated to the two farthest separated corners of the underlying regular polyhedron. In the CS model, the point masses are replaced by (charged) dielectric spheres. Here we assume that upon Coulomb explosion each fragment carries one elementary charge which is equally distributed over the respective fullerenes. In Ref. [17] it was shown that in such systems charge communication is high which is consistent with the present DFT results discussed below.

3.2. Total energy balance

Application of the energy expressions according to the PCP and CS model (see method section) allows the straightforward determination of total reaction energies for all fragmentation reactions of the following kind:

$$(C_{60})_N^{2+} \rightarrow (C_{60})_X^+ + (C_{60})_Y^+, \quad 2 \le N \le 7, \;\; X + Y = N \tag{12}$$

In Fig. 2, we compare the results from our two heuristic models with the DFT results. Altogether the two models yield a good qualitative agreement with each other and with DFT. By inspection of Fig. 2, it can be directly seen that oligomers smaller than the pentamer are thermodynamically unstable upon double vertical ionization. In general, it is well-established that Coulomb explosions are dominated by asymmetric fragmentation processes [36]. Moreover, in Ref. [35] the stability and decay channels of multiply charged fullerene clusters were investigated in particular by means of a contact sphere model. It was found that emission of a singly

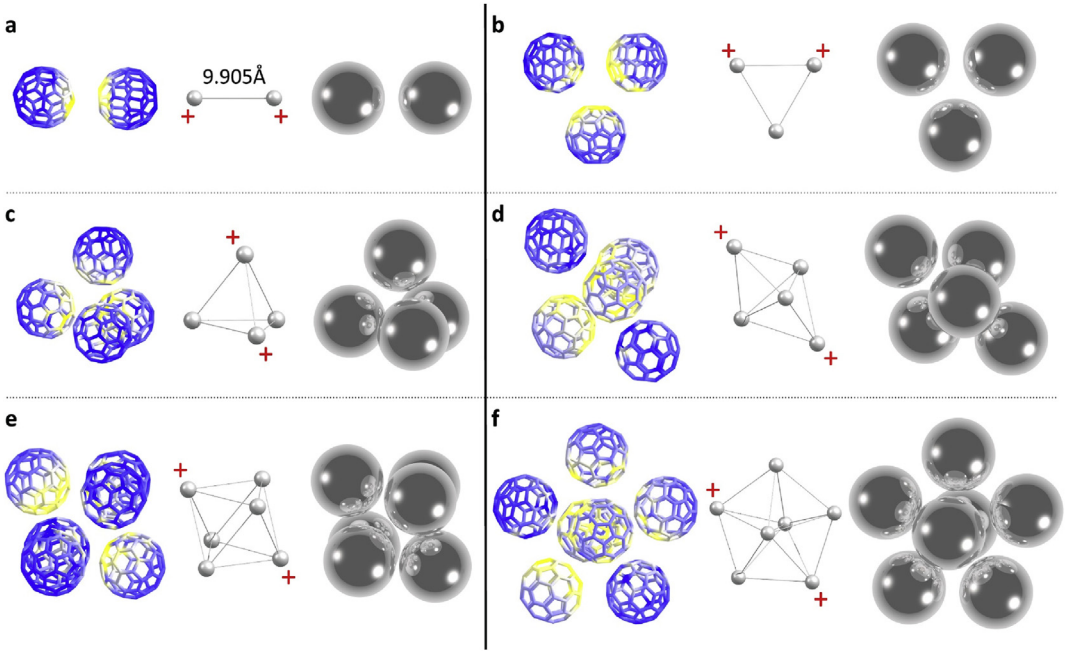

Fig. 1. Illustrations of the structures used in DFT and the PCP and CS models. Left panels: Geometries of the neutral fullerene clusters fully optimized at the PBE0/6-31G(d) level of theory including Grimme's latest empirical dispersion correction and correction for the basis set superposition error for the dimer up to the heptamer, **a**–**f**. Mulliken charges for the doubly vertically ionized clusters are indicated by color-coding (blue: positive, yellow: negative). Middle panels: Schematics for the structures used in the PCP model, in which the fullerenes are replaced by polarizable point particles. The locations of the point charges are indicated by red plus signs. The equilibrium distance of the neutral dimer is given also in **a**. Right panels: Schematics of the clusters of polarizable spheres with radius $8.6a_0$ replacing the fullerenes according to the CS model. (A color version of this figure can be viewed online.)

charged fullerene monomer is the energetically preferred fragmentation pathway. Indeed, we find that dissociation pathways that are associated with the emission of monomer cations are generally more exothermic than others. In contrast, oligomers larger than the pentamer are thermodynamically stable upon double ionization for all considered dissociation channels. However, the situation is not clear merely from an energetic point of view in case of the pentamer itself. In this case all results yield slightly negative reaction energies, i.e. they predict that the pentamers are unstable and should dissociate. It has to be noted that the geometries of the fragments for the reaction energies illustrated in Fig. 2 were obtained by sharp cuts of the optimized neutral fullerene oligomers, i.e. the fragments have been rigid. Thus, the stabilization of products on the right hand side of Eq. (12) is underestimated due to neglected geometrical relaxation, while the left hand side refers to vertical double ionization processes as they are experimentally explored [37]. Hence, our reaction energies represent a lower limit, i.e. reaction energies including geometrical relaxation shall provide higher binding energies. Nevertheless, a negative reaction energy is a necessary requirement for the fragmentation to occur, but is on its own not a sufficient measure. It is essential to investigate the kinetic stabilities of the clusters by inspecting the fragmentation pathways to disclose barriers that might prevent Coulomb explosions.

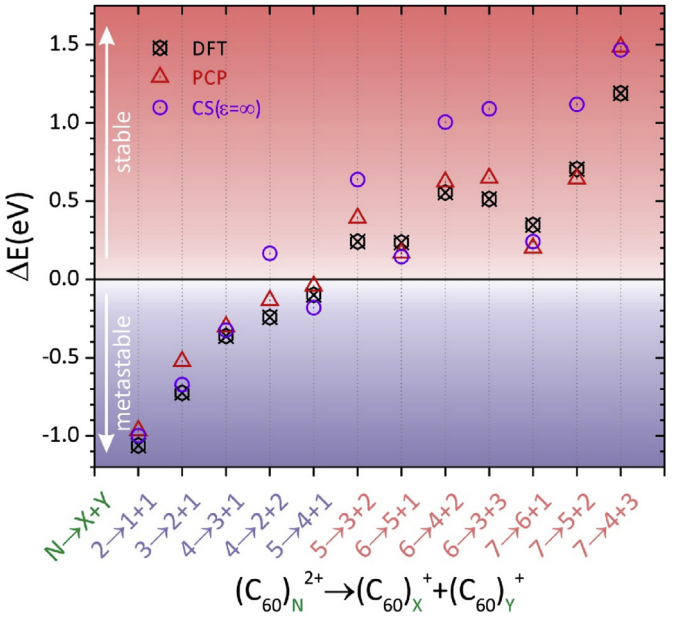

Fig. 2. Reaction energies, ΔE, for all considered fragmentation reactions, $(C_{60})_N^{2+} \rightarrow (C_{60})_X^{+} + (C_{60})_Y^{+}$, $2 \leq N \leq 7$, $X + Y = N$, computed via DFT (black, crossed hexagons), the PCP (red triangles) and the CS($\varepsilon = \infty$) (violet circles) models. Thermodynamic stability/metastability is indicated also via red/blue tick labels. This is reflected also by upper/lower half-planes shaded in red/blue, for convenience. Please note that the reaction energies do not take into account geometrical relaxation of the products; thus they actually yield lower limits for the reaction energies. (A color version of this figure can be viewed online.)

3.3. Fragmentation pathways

In order to further investigate the different dissociation pathways, we explore parts of the PESs stemming from the different methods and models. Since the most asymmetric fragmentation reactions, i.e. $(C_{60})_N^{2+} \rightarrow (C_{60})_{N-1}^{+} + C_{60}^{+}$, have the lowest dissociation energies for the dicationic systems, we restrict our investigations to these specific cases. In principle, there exists an infinite number of possible pathways on the PES resulting in (such an asymmetric) fragmentation. In the following, we refer to those pathways that are expected to exhibit the lowest barriers. In particular, in our sequential bond breaking approach, we consider the rotations and

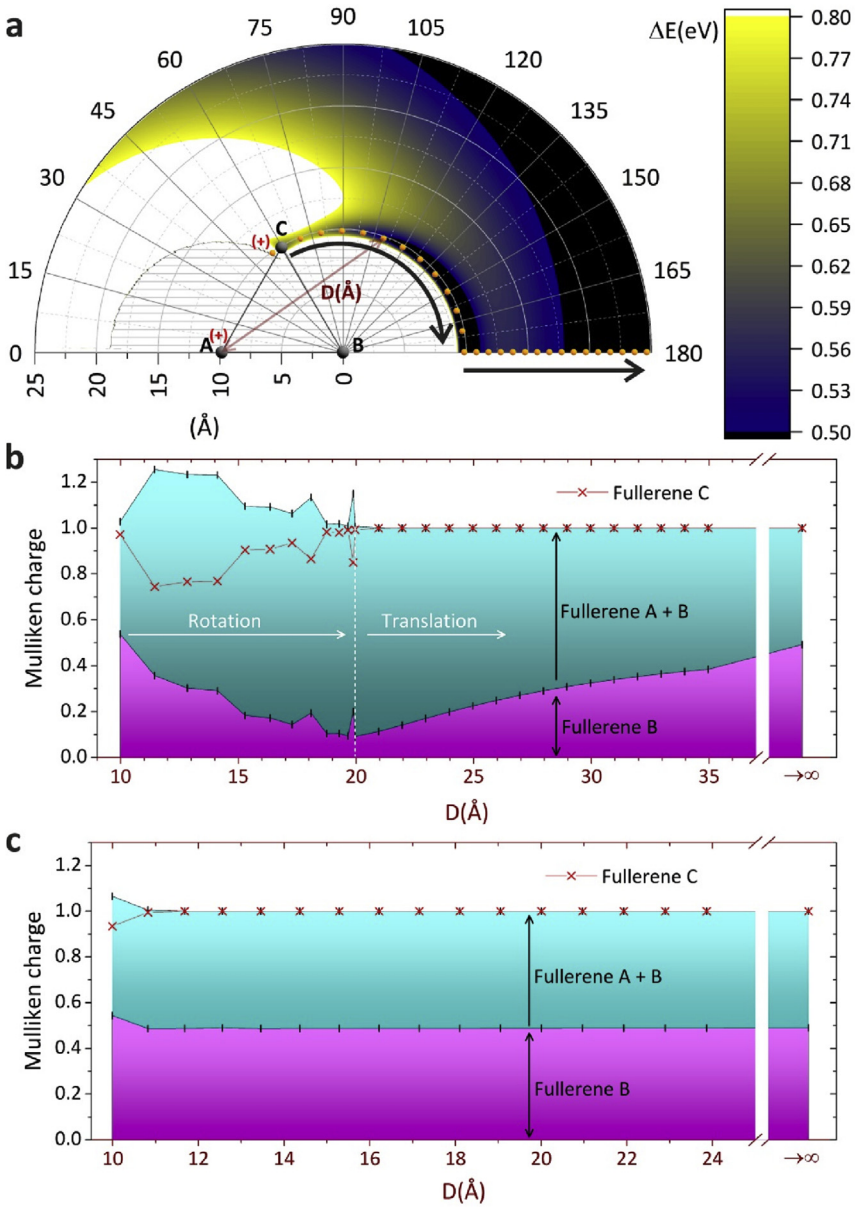

Fig. 3. **a**: Polar plot of the potential energy surface for the fullerene C as a function of the distance between the centers-of-mass of the fullerenes C and B and the angle between the centers-of-mass of the fullerenes A, B and C, while the fullerenes A and B are kept fixed in space. The energy values are derived from the CS($\varepsilon = \infty$) model. **b**: Total charges of the fullerenes A, B and C along the minimum energy pathway. **c**: Total charges of fullerenes A, B and C for the simple translation pathway described in the text and illustrated in Fig. 4a ii. (A color version of this figure can be viewed online.)

translations of one fullerene with respect to the fixed geometry of the remaining ones so that all but one of all vdW-"bonds" (for convenience we omit the quotation marks in the following) remain unchanged for any given action. For example in the case of the trimer we denote the three fullerenes as A, B, and C, see also Fig. 3a.

In the equilibrium geometry there exist three vdW-bonds A–B, B–C, C–A. Upon the first step of sequential bond breaking, the fullerenes A and B are kept fixed, while the fullerene C is rotated in the plane of the triangle around fullerene B with a fixed B–C bond length until a linear geometry is reached. Thereby the vdW-bond C–A is broken (i.e. significantly elongated) while the other two remain intact (i.e. at the equilibrium distances). In the second step, the fullerene C is translated along the axis formed by the linear A–B–C complex, resulting in breakage of the vdW-bond B–C. Up to the pentamer it is possible to follow this approach. However, due to the quadratic double pyramid shaped geometry of the hexamer, it is not possible to remove an individual fullerene without breaking at least two vdW-bonds at a time. Our approach is thus adapted such that the fewest possible vdW-bonds are broken simultaneously in one step. The rationale of the sequential bond breaking approach relies on the fact that the vdW interactions are of shortest range (following an r^{-6} dependence) among the forces present in the system. For illustration, we show in Fig. 3a a polar plot of the PES obtained with the CS model for the dissociation of the doubly charged trimer into a singly charged monomer and a singly charged dimer. Indeed, it can be seen that our above described fragmentation path is actually the lowest energy pathway. In Fig. 4a, we show schematics illustrating analogue pathways obtained via sequential bond breaking for all considered fullerene clusters, i.e. the dimer up to the pentamer (the hexamer is the first thermodynamically stable

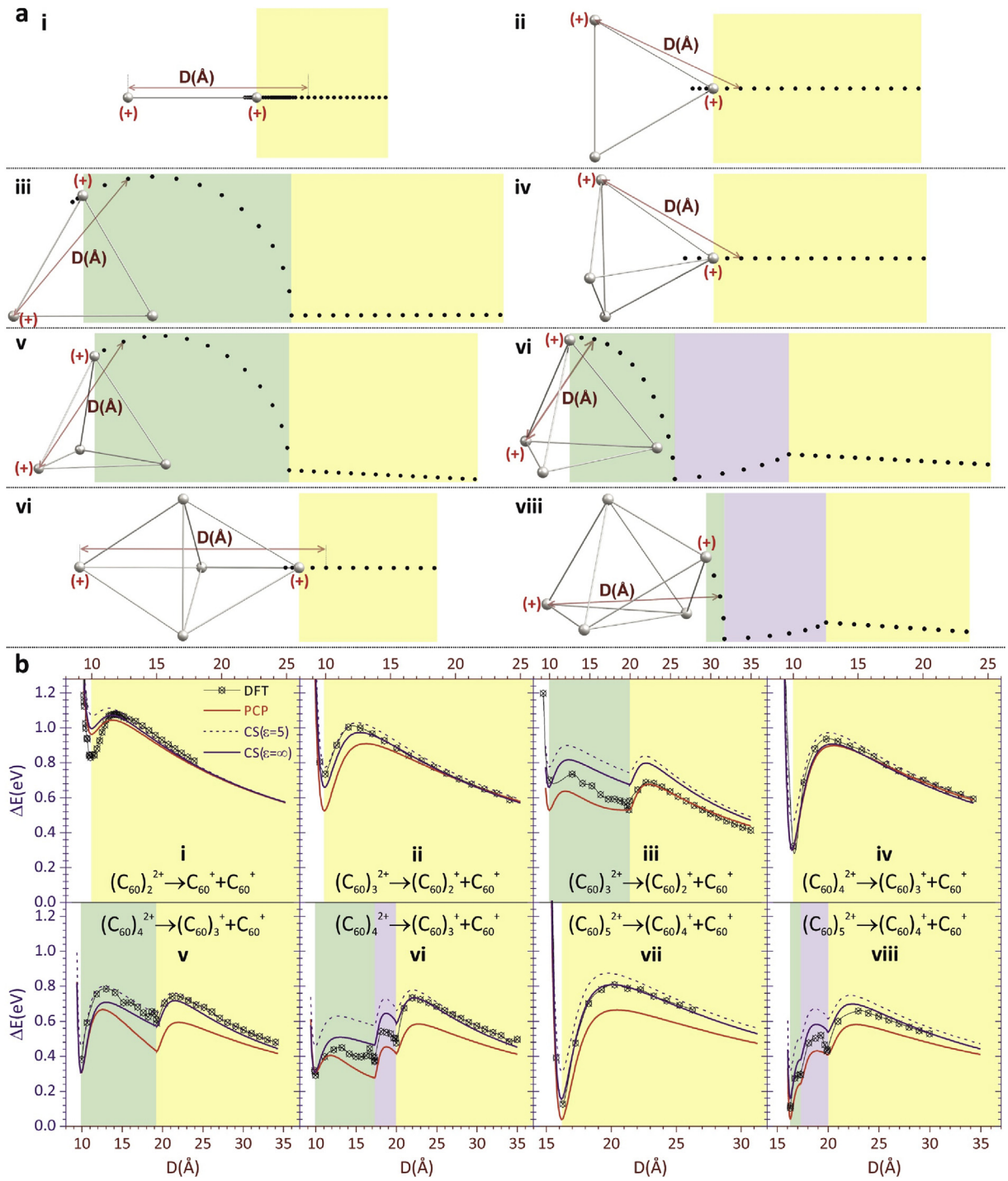

Fig. 4. **a**: Illustrations of all fragmentation pathways of the doubly charged fullerene dimer (i) to the pentamer (vii, viii) considered in this work. For a better differentiation between the different sequences in the respective fragmentation pathway, colored backgrounds are employed like follows: translational movements, first rotations, and second rotations are highlighted with a light yellow, light green, and light purple background, respectively. **b**: Potential energy scans of all fragmentation pathways considered here. Shown are energies derived via DFT (black, crossed hexagons, the black line is a guide to the eye), the PCP model (red line), and the CS model with $\varepsilon = 5$ (violet dashed line) and with $\varepsilon = \infty$ (violet solid line). (A color version of this figure can be viewed online.)

dication and therefore does not need to be investigated regarding kinetic stabilization). In these illustrations the individual sequences referring to sequential bond breaking are color-coded. In addition, we also explored alternative pathways (for which several vdW-bonds are broken simultaneously, such as a simple translation of a fullerene).

In Fig. 4a, the grey spheres correspond to the centers-of-mass of the individual fullerenes and the black circles indicate positions for which the energy of the system was evaluated with DFT along the illustrated fragmentation pathway.

In Fig. 4b, PESs are shown for all considered fragmentation pathways derived from DFT calculations and the PCP and CS models. The positions of the charges in the equilibrium structure are indicated in Fig. 4a as red plus signs (in parenthesis). One of

these point charges is then moved along the indicated path. The distance D between the two charges used as variable for the PES is also indicated in Fig. 4a. In the CS model the grey spheres in Fig. 4a correspond to the centers-of-mass of the metallic spheres by which the fullerenes are replaced in this model. To yield ideally conducting spheres, the permittivity ε was chosen to be infinite and the radius of the spheres corresponds to $8.6a_0$. It has previously been shown, that this choice of parameters can be used to successfully describe C_{60} [20]. However, there has been some controversy concerning the permittivity of individual fullerenes due to the fact that bulk fullerite yields a permittivity of up to 5 [27]. For this reason, we plot in Fig. 4b also the PESs that would be obtained by applying the CS model to fullerenes with $\varepsilon = 5$. Based on our DFT calculations, we note that the Mulliken charge distribution for small deviations from the equilibrium structures results in a reallocation of the charges with approximately one elementary charge on each of the expected fragments, i.e. C_{60}^{+} and $(C_{60})_{N-1}^{+}$ for the considered asymmetric fragmentation channels. In case of the trimer, the summed Mulliken charges of each individual fullerene as well as the respective fragments, i.e. a singly charged dimer and a singly charged monomer, are shown in Fig. 3b, along the considered fragmentation path. We note also that the charge on the larger fragment is approximately equally distributed on the fullerene constituents. This is consistent with the observed high charge communication within such systems [17,38]. Therefore, we assign for asymmetric dissociation of the $(C_{60})_{N}^{2+}$ cluster one elementary charge to the displaced fullerene monomer and e/(N−1) to the each of the N-1 remaining fullerenes in the CS model.

Concerning the fragmentation pathways shown in Fig. 4b, we first note that they all exhibit barriers that scale with both (a) the cluster size and (b) the number of vdW-bonds that are simultaneously broken in the respective dissociation process. Concerning (a), focusing for convenience now only on simple translation fragmentation processes, we find barrier heights of 0.25 eV, 0.27 eV, 0.61 eV, and 0.68 eV for dimer, trimer, tetramer, and pentamer, respectively, obtained from the DFT calculations. The given barrier heights refer to the differences between the respective barrier maxima and the local minima right in front of them. In order to exemplify point (b) we choose the case of the dicationic tetramer (Fig. 4a and b, iv-vi). The simple translation of a fullerene orthogonal to the base plane (Fig. 4a iv) results in one barrier of height 0.61 eV (Fig. 4b iv). Fig. 4b v corresponds to a two-step dissociation pathway. First a fullerene is rotated like illustrated in Fig. 4a v, which corresponds to the breakage of two vdW-bonds simultaneously yielding a barrier of 0.40 eV. Upon reaching a planar arrangement, the previously rotated fullerene is translated as shown in Fig. 4a v yielding a barrier of 0.19 eV. The overall barrier, i.e. the difference in energy of the highest barrier and the minimum corresponding to the (vertically) doubly ionized cluster in the equilibrium geometry of the neutral system (the leftmost minimum visible in the PESs depicted in Fig. 4b), corresponds to 0.40 eV. Finally, Fig. 4b vi corresponds to a three-step mechanism. In this case the fullerene is first rotated twice and then translated as shown in Fig. 4a vi. Each of these single steps corresponds to the breaking of a single vdW-bond, which corresponds to barriers of 0.16 eV, 0.21 eV, and 0.17 eV, respectively (see Fig. 4b vi). The overall barrier in this case is 0.39 eV. It is interesting to note that the overall barriers are decreasing with decreasing number of vdW-bonds broken simultaneously. This also justifies the choice of fragmentation pathways based on the sequential bond-breaking scheme. For symmetry reasons and due to the smoothness of the PESs, other fragmentation pathways are energetically between the limiting cases of the simple translation and the pathway corresponding to sequential bond breaking. The geometrical interpretation of the reduced barrier heights in the case of the latter is that before breaking all short ranged vdW-bonds, energy can be gained by adopting a better geometry with respect to the charge distribution. The simpler PCP model also illustrates this. Along the chosen lowest energy pathways, the repulsive Coulomb contribution to the energy can be significantly reduced via the involved rotations due to the increased distance between the two point charges, while at the same time the maximum contribution from the shorter-ranged attractive forces is ensured. The overall barriers obtained from DFT for the lowest energy pathways are 0.25 eV, 0.05 eV, 0.39 eV, and 0.55 eV for the dimer, trimer, tetramer, and pentamer, respectively. The key point concerning the experimentally observed stability of the dicationic pentamer is now to note that the shown PESs do not take into account geometrical relaxation of the charged systems (vertical ionization). The lower limit of the relaxation energy can be approximated as being the energy gained by the two vertical ionized fullerenes relaxing into their cationic equilibrium geometries. Thus, this energy is estimated to be (0.47 ± 0.08) eV, which exceeds the overall barriers for dimer, trimer, and tetramer, but is lower than the overall barrier for the pentamer. Hence, the pentamer dication is kinetically stabilized when formed by vertical ionization.

3.4. Comparison of methods

The qualitative agreement between the different simple models and DFT is excellent, see Fig. 4b. Both of the simple models capture the features described above. Differences can be found in the relative barrier heights and depths of the local minima. The best agreement with the DFT results can be found with the CS($\varepsilon = \infty$) model. This puts emphasis on the metallic character of the individual fullerene molecules in the cluster which was a matter of controversy in earlier studies [20–22]. The excellent agreement between the CS model and DFT is obtained by assuming that each of the two charges is evenly distributed over the respective fragmentation products. Given the simplicity of the PCP model, i.e. the reduction of the extended system to point particles, indicates nicely that these systems are dominated by basic electrostatics and dispersive interactions. For both models, the only necessary ingredient derived from DFT is the PES of the neutral dimer and the equilibrium geometries of larger neutral clusters, which could be obtained also from calculations employing accurate parametrized force fields. Both methods are simple to use and come with a negligible computational cost, yet deliver an excellent description of the considered systems.

3.5. Conclusion

We have shown that the analysis of the stability of doubly charged fullerene clusters can be effectively cut down to the interplay between classical electrostatics and dispersion interactions. The development and application of the heuristic PCP and CS approaches results in excellent agreement with DFT calculations. Based on these results, we can explain why the pentamer is the smallest doubly charged fullerene cluster ever observed [17,39]. This can be regarded as an improvement over models previously employed, such as the liquid drop model [40,41] or the contact sphere model [36], which resulted in appearance sizes of 9 and 7, respectively. Moreover, the existence of kinetic barriers also for smaller systems may in principle stabilize doubly charged fullerene clusters down to the dimer. However, for cluster sizes below the pentamer this would require highly efficient means of active cooling. The comparison of CS models employing different values for the permittivity of individual fullerenes puts further emphasis

on their metallic character. Together with recent work on the relative stability of multiply charged fullerene isomers [14], our findings open up perspectives for the systematic design and synthesis of advanced materials like man-made fullerides based on a diverse space of multiply charged fullerene cluster building blocks.

Acknowledgement

This work was supported by the Austrian Fund Agency, FWF (Vienna), via project P26635 and I987, by the Austrian Ministry of Science BMWF as part of the UniInfrastrukturprogramm of the Focal Point Scientific Computing at the University of Innsbruck, and by the Swedish Research Council (Contract No 621-2012-3660). The authors would like to acknowledge the COST action CM1204 "XUV/X-ray light and fast ions for ultrafast chemistry (XLIC)".

Appendix A. Supplementary data

Supplementary data related to this article can be found at http://dx.doi.org/10.1016/j.carbon.2016.08.056.

References

[1] A. Rotundi, F.J.M. Rietmeijer, J. Borg, Natural C_{60} and Large Fullerenes: a Matter of Detection and Astrophysical Implications, Natural Fullerenes and Related Structures of Elemental Carbon, Springer, Netherlands, Dordrecht, 2006, pp. 71–94.
[2] J.-W. Feng, H.-M. Ding, Y.-Q. Ma, Self-assembly of fullerenes and graphene flake: a molecular dynamics study, Carbon 90 (2015) 34–43.
[3] N. Martin, New challenges in fullerene chemistry, Chem. Commun. 20 (2006) 2093–2104.
[4] A.A. Popov, S. Yang, L. Dunsch, Endohedral fullerenes, Chem. Rev. 113 (8) (2013) 5989–6113.
[5] D.W. Cagle, S.J. Kennel, S. Mirzadeh, J.M. Alford, L.J. Wilson, In vivo studies of fullerene-based materials using endohedral metallofullerene radiotracers, Proc. Natl. Acad. Sci. 96 (9) (1999) 5182–5187.
[6] M. Rudolf, et al., Endohedral metallofullerenes-filled fullerene derivatives towards multifunctional reaction center mimics, Chem. A Eur. J. 18 (17) (2012) 5136–5148.
[7] Y. Iwasa, T. Takenobu, Superconductivity, Mott–Hubbard states, and molecular orbital order in intercalated fullerides, J. Phys. Condens. Matter 15 (13) (2003) R495.
[8] T.T.M. Palstra, Fullerides: superconductivity at the limit, Nat. Mater. 7 (5) (2008) 350–351.
[9] J. Cami, J. Bernard-Salas, E. Peeters, S.E. Malek, Detection of C_{60} and C_{70} in a young planetary nebula, Science 329 (5996) (2010) 1180–1182.
[10] S. Iglesias-Groth, M. Esposito, A search for near infrared bands of the fullerene cation C in the protoplanetary nebula IRAS 01005+7910, Astrophys. J. Lett. 776 (1) (2013) L2.
[11] D.K. Bohme, Multiply-charged ions and interstellar chemistry, Phys. Chem. Chem. Phys. 13 (41) (2011) 18253–18263.
[12] H. Zettergren, et al., Formations of dumbbell C_{118} and C_{119} inside clusters of C_{60} molecules by collision with a particles, Phys. Rev. Lett. 110 (18) (2013) 185501.
[13] G. Goodman, M.E. Gerschwin, D. Bercovich, Fullerene and the origin of life, Isr. Med. Assoc. J. 14 (10) (2012) 602–606.
[14] Y. Wang, S. Díaz-Tendero, M. Alcamí, F. Martín, Cage connectivity and frontier π orbitals govern the relative stability of charged fullerene isomers, Nat. Chem. 7 (11) (2015) 927–934.
[15] S. Zöttl, et al., Methane adsorption on graphitic nanostructures: every molecule counts, J. Phys. Chem. Lett. 3 (18) (2012) 2598–2603.
[16] Z. Li, Z. Liu, H. Sun, C. Gao, Superstructured assembly of nanocarbons: fullerenes, nanotubes, and graphene, Chem. Rev. 115 (15) (2015) 7046–7117.
[17] B. Manil, et al., Highly charged clusters of fullerenes: charge mobility and appearance sizes, Phys. Rev. Lett. 91 (21) (2003) 215504.
[18] A. Mauracher, et al., Formation of dianions in helium nanodroplets, Angew. Chem. Int. Ed. 53 (50) (2014) 13794–13797.
[19] S.E. Huber, A. Mauracher, On the properties of charged and neutral, atomic and molecular helium species in helium nanodroplets: interpreting recent experiments, Mol. Phys. 112 (5–6) (2014) 794–804.
[20] H. Zettergren, B.O. Forsberg, H. Cederquist, Are single C_{60} fullerenes dielectric or metallic? Phys. Chem. Chem. Phys. 14 (47) (2012) 16360–16364.
[21] A.J. Stace, E. Bichoutskaia, Treating highly charged carbon and fullerene clusters as dielectric particles, Phys. Chem. Chem. Phys. 13 (41) (2011) 18339–18346.
[22] H. Zettergren, H. Cederquist, Comment on "Treating highly charged carbon and fullerene clusters as dielectric particles" by A. J. Stace and E. Bichoutskaia, Phys. Chem. Chem. Phys., 2011, 13, 18339, Phys. Chem. Chem. Phys. 14 (48) (2012), 16770–16770.
[23] R. Antoine, et al., Direct measurement of the electric polarizability of isolated C60 molecules, J. Chem. Phys. 110 (19) (1999) 9771–9772.
[24] M. Berninger, A. Stefanov, S. Deachapunya, M. Arndt, Polarizability measurements of a molecule via a near-field matter-wave interferometer, Phys. Rev. A 76 (1) (2007) 013607.
[25] M.R. Pederson, A.A. Quong, Polarizabilities, charge states, and vibrational modes of isolated fullerene molecules, Phys. Rev. B 46 (20) (1992) 13584–13591.
[26] D.S. Sabirov, Polarizability as a landmark property for fullerene chemistry and materials science, RSC Adv. 4 (85) (2014) 44996–45028.
[27] P.C. Eklund, et al., Optical properties of C_{60}- and C_{70}-based solid films, Thin Solid Films 257 (2) (1995) 211–232.
[28] S. Grimme, S. Ehrlich, L. Goerigk, Effect of the damping function in dispersion corrected density functional theory, J. Comput. Chem. 32 (7) (2011) 1456–1465.
[29] S.F. Boys, F. Bernardi, The calculation of small molecular interactions by the differences of separate total energies. Some procedures with reduced errors, Mol. Phys. 19 (4) (1970) 553–566.
[30] C. Adamo, V. Barone, Toward reliable density functional methods without adjustable parameters: the PBE0 model, J. Chem. Phys. 110 (13) (1999) 6158–6170.
[31] T. Yanai, D.P. Tew, N.C. Handy, A new hybrid exchange–correlation functional using the Coulomb-attenuating method (CAM-B3LYP), Chem. Phys. Lett. 393 (1–3) (2004) 51–57.
[32] W.J. Hehre, R. Ditchfield, J.A. Pople, Self-consistent molecular orbital methods. XII. Further extensions of Gaussian-type basis sets for use in molecular orbital studies of organic molecules, J. Chem. Phys. 56 (5) (1972) 2257–2261.
[33] W. Branz, N. Malinowski, A. Enders, T.P. Martin, Structural transition in $(C_{60})_n$ clusters, Phys. Rev. B 66 (9) (2002) 094107.
[34] M.J. Frisch, et al., Gaussian 09, Revision D.01, Gaussian, Inc., Wallingford CT, 2009.
[35] J.M. Pacheco, J.P. Prates Ramalho, First-principles determination of the dispersion interaction between fullerenes and their intermolecular potential, Phys. Rev. Lett. 79 (20) (1997) 3873–3876.
[36] M. Nakamura, P.-A. Hervieux, Stability and fragmentation of multiply charged clusters of fullerenes, Chem. Phys. Lett. 428 (1–3) (2006) 138–142.
[37] H. Steger, J. de Vries, B. Kamke, W. Kamke, T. Drewello, Direct double ionization of C_{60} and C_{70} fullerenes using synchrotron radiation, Chem. Phys. Lett. 194 (4) (1992) 452–456.
[38] H. Zettergren, et al., Even-odd effects in the ionization cross sections of $[C_{60}]_2$ and $[C_{60}C_{70}]$ dimers, Phys. Rev. A 75 (5) (2007) 051201.
[39] H. Zettergren, et al., Stabilities of multiply charged dimers and clusters of fullerenes, J. Chem. Phys. 126 (22) (2007) 224303.
[40] O. Echt, et al., Dissociation channels of multiply charged van der Waals clusters, Phys. Rev. A 38 (7) (1988) 3236–3248.
[41] J.P.K. Doye, D.J. Wales, W. Branz, F. Calvo, Modeling the structure of clusters of C_{60} molecules, Phys. Rev. B 64 (23) (2001) 235409.